Surface mean-square displacements for NaCl

Paul D. Schulze
Department of Physics, Abilene Christian University, Abilene, Texas 79601
(Received 22 September 1975)

The mean-square displacements and mean-square velocities have been calculated for the (001) surface of a 15-layer NaCl crystal slab with the Kellermann rigid-ion and deformation-dipole models. Comparison of the two models shows that the inclusion of polarization effects results in an increase in the room-temperature value of $\langle\mu_z^2(\mathrm{Cl}^-)\rangle$ at the surface (the z direction being perpendicular to the surface) and causes the room-temperature value of $\langle\mu_z^2(\mathrm{Na}^+)\rangle/\langle\mu_z^2(\mathrm{Cl}^-)\rangle$ at the surface to depart considerably from the corresponding bulk value. The calculation of various limiting values can be determined more efficiently using Gaussian quadrature numerical integration.

In the past few years there has been interest in the vibrational properties of alkali-halide–crystal slabs.[1-4] Recently Chen *et al.*[5] have performed calculations of the surface mean-square displacements for NaCl with the Kellermann rigid-ion (KRI) model. In this paper we report the results of mean-square displacement calculations for the (001) surface of a 15-layer NaCl-crystal slab using the deformation-dipole model (DD).[6] These results are then compared to those obtained using the rigid-ion approximation.

The rigid-ion model assumes that the ions in a alkali-halide crystal interact only through closed-shell repulsion and Coulombic monopole-monopole interactions. More realistic models, such as the shell and deformation-dipole models, consider polarization effects by including monopole-dipole, dipole-dipole, etc., contributions. Chen *et al.*[7,8] have applied the shell model to the calculations of surface phonons in rocksalt-structured–crystal slabs. The deformation-dipole model has been used recently for the calculation of Schottky and Frenkel defects formation energies in alkali halides.[9] In brief, a deformation-dipole moment is the unbalanced dipole which results when the charge distribution around each ion is distorted as a result of the relative displacements of the ions against each other. These dipoles interact with the resulting dipole field from other deformed ions in addition to the Coulombic monopole field.

In the harmonic approximation, the mean-square displacements and mean-square velocities for ions in a crystal slab are given, respectively, by the expressions

$$\langle u_\alpha^2(l_3\kappa)\rangle = \frac{\hbar}{2\bar{N}M_\kappa}\sum_{\bar{q},\gamma}{}' \,|\xi_\alpha(l_3\kappa;\bar{q}\gamma)|^2 \times \frac{\coth|\hbar\omega_\gamma(\bar{q})/2k_BT|}{\omega_\gamma(\bar{q})}, \tag{1}$$

$$\langle V_0^2(l_3\kappa)\rangle = \frac{\hbar}{2\bar{N}M_\kappa}\sum_{\bar{q},\gamma}{}' \,|\xi_\alpha(l_3\kappa;\bar{q}\gamma|^2 \times \omega_\gamma(\bar{q})\coth|\hbar\omega_\gamma(\bar{q})/2k_BT| . \tag{2}$$

$\mu_\alpha(l_3\kappa)$ and $V_\alpha(l_3\kappa)$ are, respectively, the αth components of the ionic displacements and velocity associated with the κth ion in the l_3th layer of the slab. M_κ are the ionic masses and γ labels the different modes of vibration associated with one of the $\bar{N}$ allowed wave vectors $\bar{q}$ in the two-dimensional first Brillouin zone. T is the temperature and k_B is the Boltzmann constant. The eigenvalues ω and eigenvectors ξ are determined from the eigenvalue equation

$$\sum_{l_3'\kappa'\beta} D_{\alpha\beta}(l_3\kappa;l_3'\kappa';\bar{q})\xi_\beta(l_3'\kappa';\bar{q}\gamma) = \omega_\gamma^2(\bar{q})\xi_\alpha(l_3\kappa;q\gamma) , \tag{3}$$

where D is the dynamical matrix evaluated throughout the first Brillouin zone as required by Eqs. (1) and (2).

In performing the sums over $\bar{q}$ in Eqs. (1) and (2), Allen and de Wette[10] have shown that, because of the logarithmic divergence of the mean-square displacements at finite temperatures for a two-dimensional crystal as $|\bar{q}|\to 0$, one must restrict the periodicity lengths in the X and Y directions (the Z direction is taken to be normal to the slab surface) for crystals of finite thickness. As the periodicity length is allowed to be increased, the eigenfrequencies of the "acoustical" modes approach zero with the result that these frequencies dominate in Eq. (1).

In the present calculations, the sum over $\bar{q}$ has been performed by two different choices of wave vectors. For the 15-layer slabs, we have chosen the same set of 400 points in the irreducible first

zone as did Chen and co-workers.[5] This uniform grid sets the periodicity lengths, parallel to the surface, approximately equal to the slab thickness. For the bulk crystal calculations, we selected the grid of points as used in Gaussian-quadrature numerical integration.[11] This method essentially assumes an infinite supercell with the accuracy of the summation (or integration) improving as the number of Gaussian wave vectors is increased. Also, this method is computer time saving since in most wave-vector sums, as in Eqs. (1) and (2), convergence can be achieved much more rapidly than using a uniform grid of points. This method would have been ideal for the surface slabs had it not been for the unavoidable approach of $|\bar{q}| \to 0$ as the density of Gaussian wave vectors is increased. However, this method is useful in calculating ratios, such as those presented in Table I, where slab values obtained by both methods were the same to three significant figures.

In the harmonic approximation, the dynamical matrix including deformation dipoles can be written in matrix form

$$D = -M[R + A + (S + U^{-1})UHUC^{-1}(U^{-1} + \tilde{S})]M \ , \tag{4}$$

where

$$C = 1 - \alpha UHU \ .$$

R contains the short-ranged repulsive overlap interactions between first and second neighbors. H contains the long-ranged Coulomb interactions where the lattice sums were evaluated using the incomplete gamma-function transformation.[12] A is an angle-bending contribution which is due to an interaction whose potential energy is assumed proportional to the square of the angular deviation of the right angles formed by an ion and two of its nearest-neighbor dissimilar ions, i.e., $\delta U = \frac{1}{2}K(\delta\theta)^2$.[13-15] U^{-1} contains the monopole charge, M contains the ion mass, α contains the polarizability, and S contains the deformation-dipole contribution which is coupled to the monopole and dipole fields of the lattice. In this work, we have assumed deformation dipoles on anions only. Also, the dynamical matrix for the rigid-ion model is obtained by setting α, S, A, and next-nearest-neighbor interactions in R equal to zero. Explicit forms of A, S, U, α, and M are given in the Appendix.

In earlier works using the KRI, Tong and Maradudin[3] permitted both interplanar and intraplanar relaxation of ions while Chen and co-workers allowed only interplanar relaxation effects. In the present work we do not include any relaxation so that any direct comparisons between the three calculations must keep in mind their differences. Also, by using room-temperature bulk crystal force-constant parameters, we have neglected thermal-expansion effects and surface force-constant changes. Chen and co-workers[5] discuss the importance of these two effects.

Our results for the mean-square displacements $\langle \mu_\alpha^2(\kappa)\rangle$ are presented in Figs. 1–4. The values of $\langle \mu_\alpha^2(\kappa)\rangle_{DD}$ for the surface layer ($m=1$) as a function of temperature are shown in Fig. 1, while the

TABLE I. Ratio of mean-square displacements and velocities for the KRI and DD models for a 15-layer NaCl (001) crystal slab and an infinite (bulk) NaCl crystal. The Z direction is normal to the surface.

$\langle\mu_\alpha^2(\mathrm{Na}^+)\rangle/\langle\mu_\alpha^2(\mathrm{Cl}^-)\rangle$	α	T (°K)	KRI	DD
Slab	X	0 [a]	1.22	1.30
Slab	Z	0 [a]	1.21	1.20
Bulk	X, Y, Z	0 [a]	1.22	1.27
$\langle V_\alpha^2(\mathrm{Na}^+)\rangle/\langle V_\alpha^2(\mathrm{Cl}^-)\rangle$				
Slab	X	475	1.55	1.55
Slab	Z	475	1.55	1.55
Bulk	X, Y, Z	475	1.55	1.55

[a] Room-temperature parameters used in force-constant matrix.

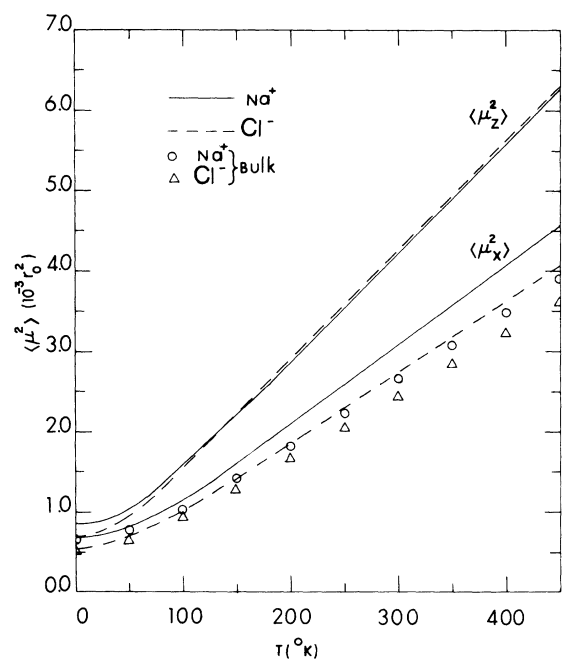

FIG. 1. Mean-square displacements $\langle\mu_\alpha^2\rangle$ for Na^+ and Cl^- ions at the surface of a 15-layer (001) crystal slab and in the bulk as a function of temperature T in the deformation-dipole model. r_0 is the distance between nearest neighbors in the bulk.

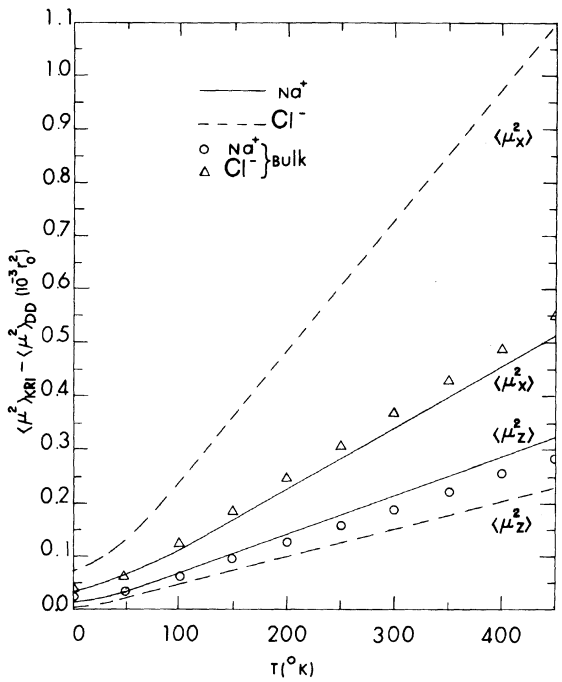

FIG. 2. Difference between the mean-square displacements calculated in the (KRI) and (DD) models, $\langle \mu_\alpha^2 \rangle_{\mathrm{KRI}} - \langle \mu_\alpha^2 \rangle_{\mathrm{DD}}$, at the surface and in the bulk as a function of temperature T.

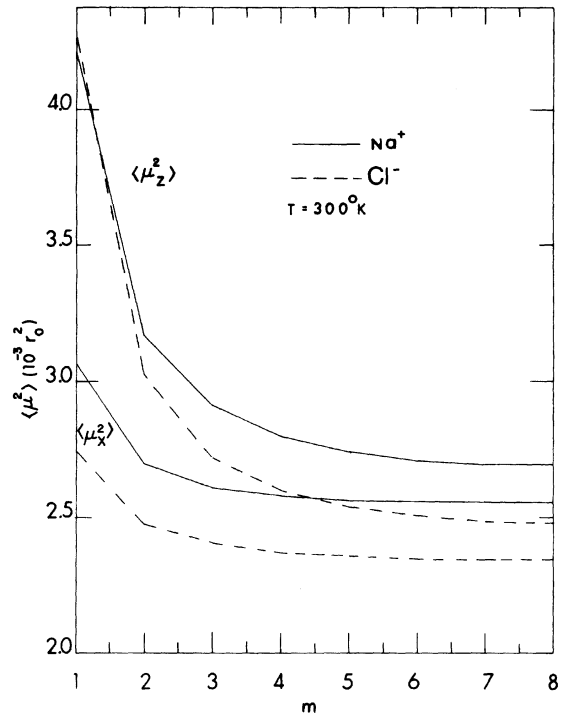

FIG. 3. Mean-square displacements $\langle \mu_\alpha^2 \rangle$ at 300 °K as a function of distance from the surface in the deformation-dipole model. Here m labels a plane of ions with $m = 1$ at the surface.

differences $\langle \mu_\alpha^2(\kappa) \rangle_{\mathrm{KRI}} - \langle \mu_\alpha^2(\kappa) \rangle_{\mathrm{DD}}$ as a function of temperature are given in Fig. 2. Figures 3 and 4 show similar results for the mean-square displacements as in Figs. 1 and 2 but this time as a function of the slab layer (m) at $T = 300$ °K. The bulk mean-square displacements obtained by using a 30-point (in the irreducible zone) Gaussian-quadrature integration are also shown for comparison purposes in Figs. 1 and 2. The room-temperature values at the center of the slab ($m = 8$) are to within a few percent of the corresponding bulk values, thus indicating that the periodicity lengths parallel to the slab surface were chosen about right in order that the surface values obtained in this work are indicative of the surface values for a thick crystal.[10]

The surface mean-square displacements are larger than the corresponding bulk values with $\langle \mu_z^2(\kappa) \rangle_{\mathrm{surface}} / \langle \mu_z^2(\kappa) \rangle_{\mathrm{bulk}}$ reaching a room-temperature value of 1.61 for Na^+ and 1.75 for Cl^-. Chen and co-workers[5] obtained a value of 1.6 for both ions. Since the force-constant matrix used in the present work is not invariant under interchange of Na^+ and Cl^- ions because of the next-nearest repulsive interactions and lack of deformation dipoles on cations, the mean-square displacements of the two ions will not be equal in the high-temperature limit. On the other hand, the force-con-

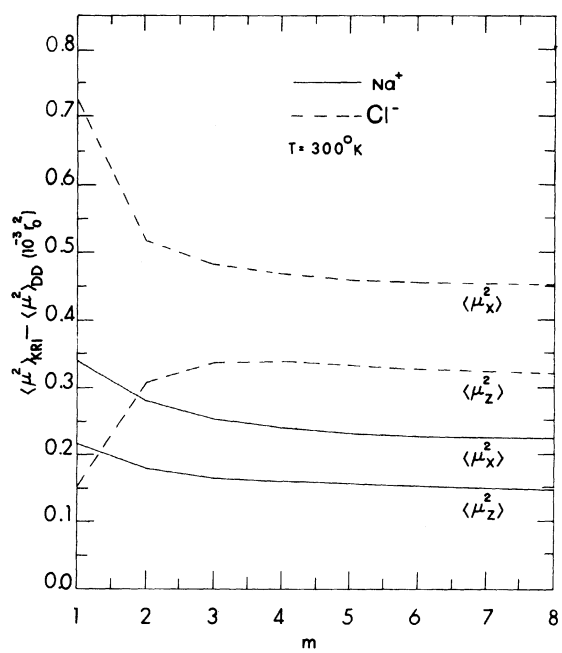

FIG. 4. Difference between the mean-square displacements calculated in the KRI and DD models at 300 °K as a function of distance from the surface.

stant matrix used in the rigid-ion approximation was invariant in the manner described above and the mean-square displacements were observed to converge in the high-temperature limit.

As indicated in Fig. 2, the mean-square displacements calculated using the rigid-ion model were found to be larger than the corresponding values calculated in the deformation-dipole approximation. This would seem to indicate that polarization and next-nearest-neighbor interactions, which are both repulsive, lower the amplitudes of vibration. Musser[16] found similar reductions in the mean-square displacements of monatomic metals as the force constants were increased. Musser found that if the force constants between nearest neighbors in the surface plane were increased, there resulted a greater decrease in the mean-square displacement component parallel to the surface than for the perpendicular component. Observation of Fig. 2 shows that $\langle \mu_x^2 \rangle_{\mathrm{KRI}} - \langle \mu_x^2 \rangle_{\mathrm{DD}}$ is larger than for the perpendicular component. This would seem to be in agreement with Musser's work because the surface anions have no deformation-dipole moment normal to the surface resulting in a lowering of the effective interplanar force constant relative to the effective intraplanar force constant.

A study of the mean-square displacements as a function of layer m (see Figs. 3 and 4) revealed two main differences between the rigid-ion and deformation-dipole models. The first of these is shown in Fig. 3 for the surface layer ($m=1$). The values of $\langle \mu_x^2 \rangle$ for the two ions are widely separated whereas they are nearly equal in the rigid-ion calculations. This can also be seen in Fig. 1 at $T=300\,^\circ\mathrm{K}$ and is due to the variance of the force-constant matrix under interchange of ions as mentioned above. The second difference is the crossover which occurs at the fifth layer ($m=5$) as seen in Fig. 3. No such crossover was found for the rigid-ion model.

In Fig. 4 we see that the most drastic change in $\langle \mu_\alpha^2 \rangle_{\mathrm{KRI}} - \langle \mu_\alpha^2 \rangle_{\mathrm{DD}}$ occurs between the surface ($m=1$) and second ($m=2$) layers for the Cl^- ion which contains the deformation dipoles. Then as one moves to deeper layers, the differences for all the ions remains essentially a constant. This large variation seen at the surface may again be due to the relative weakening of the effective interplanar force constants over their intraplanar counterparts. No such missing dipoles are present on subsurface ions.

As a final comparison between the deformation-dipole and KRI models, we would like to consider some limiting cases which are presented in Table I. The values listed for the mean-square displacement ratios $\langle \mu_\alpha^2(\mathrm{Na}^+) \rangle / \langle \mu_\alpha^2(\mathrm{Cl}^-) \rangle$ in the rigid-ion approximation turned out to be the same as those obtained by Chen and co-workers[5] who allowed interplanar displacements.[17] Again the most significant difference between the two models is for the mean-square displacement component parallel to the surface. However, it is the normal component in the deformation-dipole approximation which departs most significantly from the bulk value in the same approximation. As indicated in Table I, the ratios $\langle V_\alpha^2(\mathrm{Na}^+) \rangle / \langle V_\alpha^2(\mathrm{Cl}^-) \rangle$ were all found to have the value of 1.55 regardless of the model used or whether the ions were on the surface of the slab or in bulk crystal. The equipartition of energy can be expressed as

$$\tfrac{1}{2} M_\kappa \langle V_\alpha^2(l_3\kappa) \rangle^2 = \tfrac{1}{2} k_B T \text{ for } T \to \infty$$

for all κ, α, and l_3. Thus

$$\langle V_\alpha^2(l_3\mathrm{Na}^+) \rangle / \langle V_\alpha^2(l_3\mathrm{Cl}^-) \rangle = (M_{\mathrm{Na}^+}/M_{\mathrm{Cl}^-})^{-1} = 1.54\,.$$

The value of 1.55 obtained in this work is slightly high because of the finite temperature; however, the value does show the independence of this ratio upon the model. A final note, in connection with the values given in Table I, is that these ratios were found to be independent of the method used in summing over the two-dimensional Brillouin zone. This means that the ratios for different slab models can be compared with a considerable saving of computer time by using Gaussian-quadrature numerical integration as was done for the bulk crystal.

Even though the mean-square displacements represent averages over all the vibrational modes and thus should not be too sensitive to the specifics of the vibrational spectrum, some differences between the KRI and deformation-dipole models were observed in this work. Also, as Chen and co-workers[5] have indicated, the "acoustical" modes in Eq. (1) contribute heavily to the averages and since these modes are described well by a rigid-ion model, one would not expect great differences in the results for the two models. Nevertheless, we found that differences were present even though the qualitative features of the two calculations were similar. In summary, two notable differences were the larger values of 1.75 for $\langle \mu_z^2(\mathrm{Cl}^-) \rangle_{\mathrm{surface}} / \langle \mu_z^2(\mathrm{Cl}^-) \rangle_{\mathrm{bulk}}$ at $300\,^\circ\mathrm{K}$ and 1.30 for $\langle \mu_x^2(\mathrm{Na}^+) \rangle / \langle \mu_x^2(\mathrm{Cl}^-) \rangle$ at $0\,^\circ\mathrm{K}$ in the deformation-dipole approximation. Perhaps even more significant, was the large departure of $\langle \mu_z^2(\mathrm{Na}^+) \rangle / \langle \mu_z^2(\mathrm{Cl}^-) \rangle$ from the corresponding $0\,^\circ\mathrm{K}$ value calculated for the bulk crystal. In the rigid-ion approximation, both slab components were found to be close to the corresponding bulk value. Since a model which includes polarization effects gives an overall better description of the vibrational spectra of alkali halides, the bulk value of 1.27 calculated using the

deformation-dipole model should be more reliable.[18] Although the effects of thermal expansion, intraplanar and interplanar expansion, and surface force-constant changes are important for a realistic surface slab model, they were considered to be out of the scope of the present work. We have shown that the deformation-dipole model is feasible for surface calculation; however, a detailed study is being planned to include the above-mentioned effects.

The author wishes to express his gratitude to Dr. T. S. Chen, Dr. G. P. Alldredge, and Dr. F. W. de Wette for the use of their routine to calculate the Coulomb lattice sums and for the many helpful discussions with Dr. Alldredge. The author also wishes to thank the Robert A. Welch Foundation of Houston, Texas and the Research Council at Abilene Christian University for their support of this work, and Research Corporation for their original support of the project.

APPENDIX: ELEMENTS OF THE DYNAMICAL MATRIX

The elements $R_{\alpha\beta}(l_3\kappa p; l_3'\kappa' p'; \bar{q})$ [cf. Eq. (4)] are given in Ref. 3 while the elements $H_{\alpha\beta}(l_3\kappa p; l_3'\kappa' p'; \bar{q})$ are those used by Chen.[19] Here p denotes the parity. In the following, a superscript s will denote a surface layer exclusively.

A. Elements U, M, and α

Let e_κ, m_κ, and α_κ be, respectively, the electronic charge, the ionic mass, and the atomic polarizability. Then

$$U \equiv \delta_{\alpha\beta}\delta_{\kappa\kappa'}\delta_{l_3 l_3'}/e_\kappa ,$$

$$M \equiv \delta_{\alpha\beta}\delta_{\kappa\kappa'}\delta_{l_3 l_3'}/m_\kappa^{1/2} ,$$

and

$$\alpha \equiv \delta_{\alpha\beta}\delta_{\kappa\kappa'}\delta_{l_3 l_3'}\alpha_\kappa .$$

B. Angle-bending elements A

Let the constant C' be defined[15]

$$C' = r_0^4(C_{44} - C_{12})/e^2 ,$$

where r_0 is the distance between nearest neighbors in the bulk and C_{12} and C_{44} are the elastic constants. Given below are the nonzero angle bending elements including the ionic masses in Eq. (4).

Case (i). $\kappa \neq \kappa'$; $p = p'$; $C = C'/m_\kappa$:

$$A_{xx} = A_{yy} = A_{zz} = 8C ,$$

$$A_{xy} = A_{yx} = 2C \sin\bar{q}_x r_0 \sin\bar{q}_y r_0 ,$$

$$A_{xx}^s = A_{yy}^s = 6C ,$$

$$A_{zz}^s = 4C ,$$

$$A_{xy}^s = A_{yx}^s = A_{xy} .$$

Case (ii). $\kappa \neq \kappa'$; $p = p'$; $C = C'(m_\kappa m_{\kappa'})^{-1/2}$:

$$A_{xx} = -4C \cos\bar{q}_y r_0 ,$$

$$A_{yy} = -4C \cos\bar{q}_x r_0 ,$$

$$A_{zz} = 2A_{zz}^s = A_{xx} + A_{yy} ,$$

$$A_{xz}^s = -A_{zx}^s = iC(\delta_{l_3,1} - \delta_{l_3,15}) \sin\bar{q}_x r_0 ,$$

$$A_{yz}^s = -A_{zy}^s = iC(\delta_{l_3,1} - \delta_{l_3,15}) \sin\bar{q}_y r_0 .$$

Case (iii). $\kappa = \kappa'$, $p \neq p'$; $C = C'/m_\kappa$:

$$A_{xz} = A_{zx} = iC(\delta_{l_3,l_3'-1} - \delta_{l_3,l_3'+1}) \sin\bar{q}_x r_0 ,$$

$$A_{yz} = A_{zy} = iC(\delta_{l_3,l_3'-1} - \delta_{l_3,l_3'+1}) \sin\bar{q}_y r_0 .$$

Case (iv). $\kappa \neq \kappa'$, $p \neq p'$; $C = C'(m_\kappa m_{\kappa'})^{-1/2}$;

$$A_{xx} = A_{yy} = -2C(\delta_{l_3,l_3'-1} + \delta_{l_3,l_3'+1}) .$$

C. Deformation-dipole matrix elements S

Consider the following definitions[6]:

$$\gamma_{Na^+} = \gamma'_{Na^+} = 0 ,$$

$$\gamma_{Cl^-} = \tfrac{1}{2} e(z - z^*)(r_0/\rho - 2)^{-1} ,$$

$$\gamma'_{Cl^-} = -r_0 \gamma_{Cl^-} \rho^{-1} ,$$

where z^* is the effective electronic charge and ρ is the Born-Mayer short-range repulsive potential screening parameter. Also, let

$$\delta_{i;j,k} = \begin{cases} 1 \text{ if } i = j \text{ or } k \\ 0 \text{ otherwise} . \end{cases}$$

Then

$$S_{\alpha\beta}(l_3\kappa, l_3'\kappa'; \bar{q}) = -b_\alpha^{l_3}(\kappa)\delta_{\alpha\beta}\delta_{\kappa\kappa'}\delta_{l_3,l_3'} + \sum_{m=0,\pm1} a_\alpha^{l_3+m}(\kappa')\delta_{\alpha\beta}(1 - \delta_{\kappa\kappa'})\delta_{l_3+m,l_3'} ,$$

where

$$b_\alpha^{l_3}(\kappa) = \gamma'_\kappa(2 - \delta_{l_3;1,15}\delta_{\alpha,z}) + \gamma_\kappa(4 - \delta_{l_3;1,15}\delta_{\alpha;x,y}) ,$$

$$a_\alpha^{l_3}(\kappa) = 2[\gamma'_\kappa(1 - \delta_{\alpha,z}) \cos\bar{q}_\alpha r_0 + \gamma_\kappa(\cos\bar{q}_\lambda r_0 + \delta_{\alpha,z} \cos\bar{q}_\epsilon r_0)] ,$$

$$a_\alpha^{l_3-1}(\kappa) = (1 - \delta_{l_3,1})[\gamma'_\kappa \delta_{\alpha,z} + \gamma_\kappa(1 - \delta_{\alpha,z})] ,$$

$$a_\alpha^{l_3+1}(\kappa) = (1 - \delta_{l_3,15})[\gamma'_\kappa \delta_{\alpha,z} + \gamma_\kappa(1 - \delta_{\alpha,z})] .$$

In the second equation α, ϵ, and λ correspond to x, y, and z and are all different with $\lambda \neq z$.

[1]R. Fuchs and K. L. Kliewer, Phys. Rev. 140, A2076 (1965).
[2]A. A. Lucas, J. Chem. Phys. 48, 3156 (1968).
[3]S. Y. Tong and A. A. Maradudin, Phys. Rev. 181, 1318 (1969).
[4]W. E. Jones and R. Fuchs, Phys. Rev. B 4, 3581 (1971).
[5]T. S. Chen, G. P. Alldredge, and F. W. de Wette, Phys. Rev. B 6, 623 (1972).
[6]J. R. Hardy, Philos. Mag. 7, 315 (1962).
[7]T. S. Chen, G. P. Alldredge, and F. W. de Wette, Solid State Commun. 10, 941 (1972).
[8]T. S. Chen, G. P. Alldredge, and F. W. de Wette, Phys. Lett. A 40, 401 (1972).
[9]P. Schulze and J. R. Hardy, Phys. Rev. B 5, 3270 (1972).
[10]R. E. Allen and F. W. de Wette, Phys. Rev. 179, 873 (1969).
[11]L. L. Boyer and J. R. Hardy, Phys. Rev. B 4, 1079 (1971).
[12]T. S. Chen, R. E. Allen, G. P. Alldredge, and F. W. de Wette, Solid State Commun. 8, 2105 (1970). Also see an erratum: *ibid.* 9, No. 16, xi (1971).
[13]P. S. Yuen and Y. P. Varshni, Phys. Rev. 164, 895 (1967).
[14]B. C. Clark, D. C. Gazis, and R. F. Wallis, Phys. Rev. 134, 1486 (1964).
[15]S. S. Jaswal and J. R. Hardy, Phys. Rev. 171, 1090 (1968).
[16]S. W. Musser, J. Phys. Chem. Solids 32, 115 (1971).
[17]It will be interesting to see if this happens when we allow interplanar displacements using the deformation-dipole model.
[18]See Table I of Ref. 5 for other values.
[19]T. S. Chen, Ph.D. dissertation (University of Texas, 1971) (unpublished). See also Refs. 5 and 12.